American Journal of Ophthalmology Case Reports 19 (2020) 100757

Contents lists available at ScienceDirect

American Journal of Ophthalmology Case Reports

journal homepage: www.elsevier.com/locate/ajoc

On the axial location of Gunn's dots

Daniel X. Hammer[a,*], Zhuolin Liu[a], Jenna A. Cava[b], Joseph Carroll[b], Osamah Saeedi[c]

[a] Division of Biomedical Physics, Office of Science and Engineering Laboratories, Center for Devices and Radiological Health, Food and Drug Administration, 10903 New Hampshire Avenue, Silver Spring, MD, 20993, USA
[b] Department of Ophthalmology and Visual Sciences, Medical College of Wisconsin, 925 N. 87th Street, Milwaukee, WI, 53226, USA
[c] Department of Ophthalmology and Visual Sciences, University of Maryland School of Medicine, 419 W. Redwood Street, Baltimore, MD, 21201, USA

ARTICLE INFO

Keywords:
AO-OCT
AOSLO
Gunn's dots
Hyalocyte
Microglia
Müller cells

ABSTRACT

Purpose: To determine the axial location of Gunn's dots in the retina.
Methods: Adaptive optics scanning laser ophthalmoscopy (AOSLO) images and adaptive optics – optical coherence tomography (AO-OCT) volumes were collected from a region where Gunn's dots were found inferior to the optic disc from a subject determined by clinical examination to be a glaucoma suspect. AO-OCT volumes were also collected along the horizontal and vertical meridians from six healthy subjects and one glaucoma subject to identify and document other occurrences of Gunn's dots. AO-OCT volumes were registered in three-dimensions and averaged. Gunn's dots were segmented, and their volume, area, and diameter were measured.
Results: All Gunn's dots imaged in this study from all subjects were confined to the inner limiting membrane, neither extending into the vitreous nor into the nerve fiber layer. The size of the dots was highly variable. The measured volume, area, and diameter (mean ± standard deviation) were 1119.9 ± 590.9 μm^3, 220.2 ± 105.5 μm^2, and 14.3 ± 3.1 μm, the latter within the range as previously published reports.
Conclusions: Based upon evidence from this study and others, Gunn's dots are not thought to be Müller cell end-feet or hyalocytes. We hypothesize that they are related to microglia, either as the by-product of their phagocytosis function, or are actual dead ameboid-shaped microglia who have fulfilled their scavenger role in retinal pathology. Further studies are needed in diseased eyes to determine if they have predictive value.

1. Introduction

Gunn's dots are hyperreflective retinal structures whose origin, function, and relationship to pathology are yet to be unambiguously determined.[1] Two recent studies using color and red-free fundus photography and high-resolution adaptive optics (AO) fundus imaging have shed new light on their characteristics.[2,3] They are highly prevalent in adolescent eyes and, though stable over months to years, their density apparently decreases with age. In adolescents, they are preferentially distributed in regions of thickened nerve fiber layer (NFL) superior and inferior to the optic disc,[3] though in adults they may be found more uniformly distributed in the macula.[2] Their occurrence is more likely in adolescents with dark irises compared to blue irises.[3] The reflectance of Gunn's dots is highly sensitive to illumination angle of incidence.[2] It has been hypothesized that Gunn's dots are either Müller cell end-feet or hyalocytes.[2–4] Müller cells are glial cells that extend from the inner limiting membrane (ILM) to the outer limiting membrane (OLM) providing several functions related to metabolism, homeostasis, neural protection, and waste phagocytosis.[5] Hyalocytes are macrophages in the vitreous cavity that are responsible for extracellular matrix synthesis and modulation of vitreous immune response and inflammation.[6]

While these recent studies have improved our understanding of Gunn's dots, fundamental questions remain regarding their origin, function, and relation to pathology. The purpose of this study was to use the precise depth-sectioning capabilities of AO-OCT to determine the axial location of Gunn's dots. High resolution depth sectioning of Gunn's dots is also expected to shed light on their relationship to retinal glial cells, which in turn may provide further clues as to their origin and function.

2. Materials and methods

2.1. Patients and AO imaging

A single patient, determined by clinical examination by a trained glaucoma specialist to be a glaucoma suspect, was imaged on the Medical College of Wisconsin AOSLO instrument[7,8] and the FDA multimodal AO imager[9] as part of glaucoma studies at both sites. The

* Corresponding author.
E-mail address: daniel.hammer@fda.hhs.gov (D.X. Hammer).

https://doi.org/10.1016/j.ajoc.2020.100757
Received 18 November 2019; Received in revised form 13 May 2020; Accepted 24 May 2020
Available online 01 June 2020

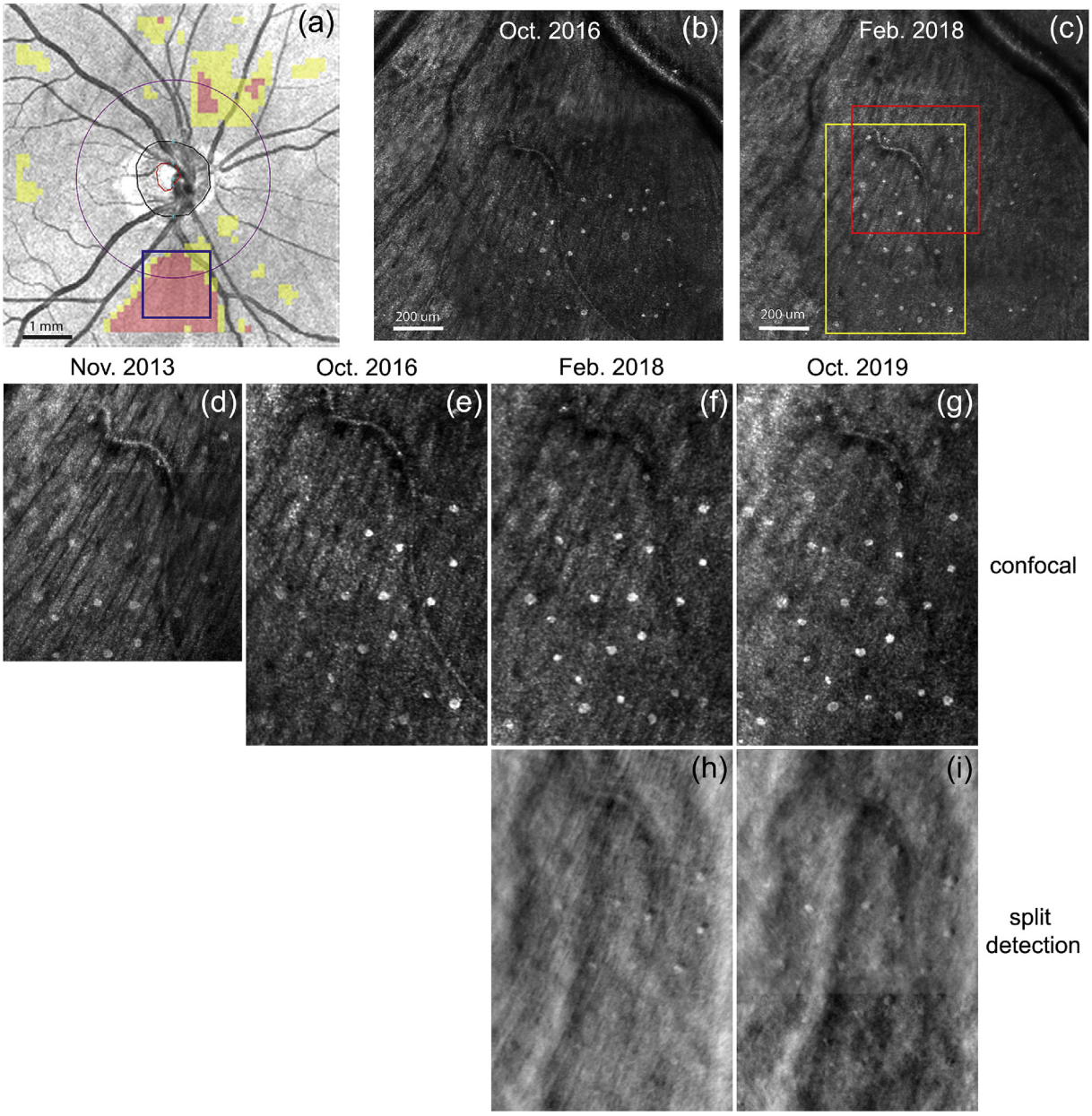

Fig. 1. AOSLO images of Gunn's dots in the inferior nasal region of a 43-year-old glaucoma suspect subject. (a) Clinical OCT scan with overlay showing regions of NFL thinning (in pink) inferior to the disc where the AOSLO data were acquired (blue box). (b–c) Two AOSLO montages taken at timepoints separated by ~16 months. Yellow box indicates region shown in (d–i). Red box indicates region where AO-OCT volumes were collected in Apr. 2019. (d–g) Confocal and (h–i) split detection AOSLO images at four imaging sessions separated by ~6 years showing stability of Gunn's dots. (For interpretation of the references to color in this figure legend, the reader is referred to the Web version of this article.)

subject was known from previous retinal examination to have Gunn's dots in a region below the optic nerve head (Fig. 1(a)).[10] Additional subjects (n = 7, six healthy subjects and one glaucoma patient) were imaged at the FDA to identify occurrences of Gunn's dots along the horizontal and vertical meridians. All subjects were consented according to human subject protocols approved by the Medical College of Wisconsin and FDA Institutional Review Boards in accordance with the principles of the Declaration of Helsinki.

Confocal and dark field AOSLO images (1.5° × 1.5° field-of-view), spanning ~4-5° and located ~5° inferior and ~12° nasal to the fovea, were collected, registered, averaged, and montaged as shown in Fig. 1(b) and (c). AO-OCT volumes (n = 300) sized 1.5° × 1.5° were collected from a single location in the same region and were registered in three dimensions and averaged. The AOSLO and AO-OCT system focus was pulled to the inner retina at approximately the level of the NFL during image acquisition. In order to document the presence of Gunn's dots in the macula, AO-OCT volumes (n = 30) sized 1.5° × 1.5° and spaced 1.5° were collected across the horizontal and vertical meridians. The data were used in this report to compare Gunn's dots from the primary nasal location in the glaucoma suspect patient to those observed at other retinal locations in other healthy control subjects.

2.2. Segmentation and sizing

A 3-D registration algorithm with sub-cellular accuracy was used to register and average AO-OCT volumes that were collected at each retinal location. Gunn's dots in the averaged AO-OCT volumes were then segmented and sized with a custom three-dimensional segmentation algorithm as follows. First, the average volume was aligned axially (i.e., flattened) to the ILM. The volume was then manually cropped to a

region 30-pixels (20.6-μm) deep encompassing the ILM. Next, each cropped B-scan from the volume was thresholded and passed through a particle filter (retaining dots sized > 10 depth pixels) to segment the Gunn's dots in depth. Gunn's dots identified from adjacent B-scans were grouped within a lateral position tolerance (center-of-mass within 5 pixels) and further filtered laterally (retaining dots sized > 3 lateral pixels). Finally, the Gunn's dot volume was quantified by summing all pixels corresponding to each dot. A summed depth projection (maximum intensity projection) of the thresholded volume was also created to compare to previously published area and diameter measurements from traditional retinal imaging. Owing to the interaction between threshold level and particle filter size, the algorithm gave more rigorous segmentation of Gunn's dots in the cross-sectional plane compared to *en-face* plane within the OCT volume.

3. Results

Figure 1 shows AOSLO confocal images from the glaucoma suspect patient over the course of four sessions separated by six years. The pattern of the Gunn's dots in Fig. 1(d–g) indicate they were stable over six years in this subject, consistent with previous reports.[2] The split detection AOSLO images in Fig. 1(h–i) show signal from the Gunn's dots, but their appearance suggests strong light directionality. The slight difference in appearance of individual Gunn's dots between images is probably due to slight differences in light directionality (pupil position) or system focus between sessions. While AOSLO can provide much higher resolution images of the Gunn's dots than traditional clinical images or previous non-confocal AO fundus imaging, the axial location and extent is still ambiguous.[2,11]

Figure 2 shows AO-OCT images of Gunn's dots taken from the same location shown in Fig. 1(c) (red box). *En-face* slices through the ILM, just below the ILM (8.2 μm below ILM), at the middle of the NFL (25.3 μm below ILM) and at the base of the NFL (49.3 μm below ILM) are shown in Fig. 2(a–d). Vertical and horizontal cross-sections through two Gunn's dots are shown in Fig. 2(e–f). Results of the three-dimensional segmentation algorithm are shown in the cross-sectional and *en-face* slides in Fig. 2(g–i). The mean volume, area (flattened in depth), and maximum Ferret diameter of the Gunn's dots in Fig. 2 were measured to be 1119.9 μm^3 (± 590.9 stdev, range: 252.3–2681.3), 220.2 μm^2 (± 105.5 stdev, range: 67.7–497.5), and 14.3 μm (± 3.1 stdev, range: 8.9–20.6). The latter is very similar to the 13.3 ± 3.5 reported previously.[2] The density is 89.2 mm^{-2}, which is also in line with the density distribution with age shown in that paper. The *en-face* section through the ILM (Fig. 2(a)) also shows evidence of additional hyperreflective structures and possibly the presence of microglia (arrow) at the ILM.

For the AO-OCT volumes collected along the horizontal and vertical meridians, Gunn's dots were found at relatively low density (a single dot observed in both meridians) in 4 of 6 healthy subjects. Gunn's dots were found at significantly higher density in the macula of the glaucoma suspect subject than the healthy subjects (20 total dots observed in both meridians for all subjects). Figure 3 shows AO-OCT images of Gunn's dots found in four healthy subjects at various locations along the meridians. The Gunn's dots in the macula were typically smaller than those found in other retinal locations.

To study the potential relationship between Gunn's dots and microglia, as well as other structures near the ILM, we also reviewed data from our healthy and glaucoma subjects that may reveal clues of the origin and function of Gunn's dots. Figure 4 shows imaged regions from a healthy subject with relatively dense ILM microglia (Fig. 4(a)), from a healthy subject with several microglia in various activation stages (Fig. 4(b)), from a healthy older subject with moderate hyperreflective regions of unknown cellular origin (Fig. 4(c)), and from an advanced glaucoma subject with substantial hyperreflective regions at the ILM (Fig. 4(d)). The cellular debris-like structures may be part of the formation of epiretinal membranes (or activated retinal astrocytes and Muller cells – ARAM) in glaucoma and healthy subjects.

4. Discussion

The high AO-OCT axial resolution (~4 μm) provides unambiguous determination of the depth location of Gunn's dots within the ILM layer. They neither reside in the vitreous above the ILM nor does the hyperreflective portion extend into the NFL or inner plexiform layer (IPL, Figs. 2 and 3). Quantification of the diameter and area matches previous measurements and AO-OCT imaging allows measurement of their volume. Their size, shape, and density are highly variable, also in agreement with recent imaging studies.[2]

While their diameter may match that of Müller cell end-feet at the ILM (~5–15 μm),[12] several characteristics probably rule out Gunn's dots as the manifestation of Müller cell end-feet. First, the posterior portion of Gunn's dots do not exhibit the funnel or conical shape noted in histological sections of Müller cells.[12] At their widest point, all of the Gunn's dots examined in this study are disc-shaped in depth, with the anterior and posterior segment perimeters roughly equivalent. Second, there is no evidence that the Gunn's dots connect to a stalk in the IPL, which in turn projects to a soma in the INL. It is possible that the diameter of a Müller cells stalk (~3 μm) and its refractive index are

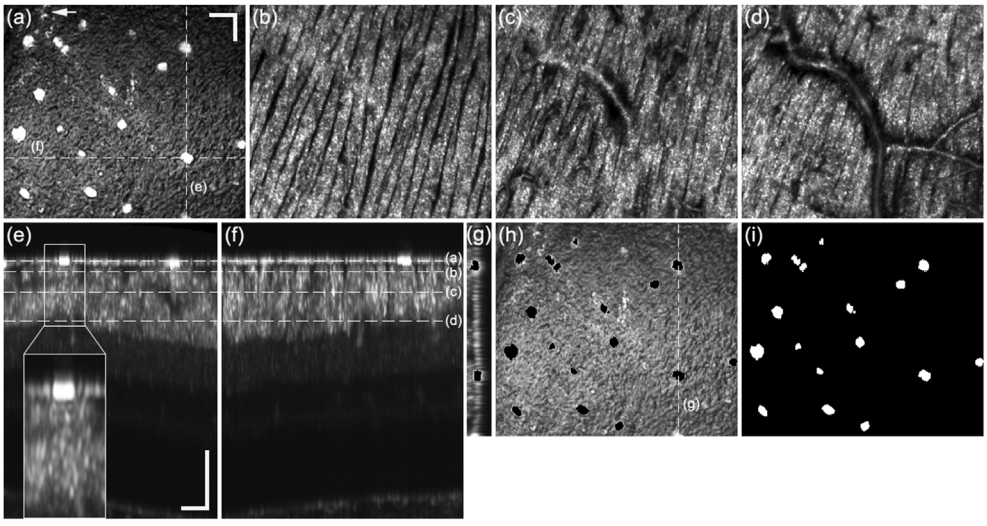

Fig. 2. AO-OCT imaging of Gunn's dots in inferior nasal region of a glaucoma suspect patient. (a) *En-face* slice at ILM. Dashed lines show location of cross-sectional scans shown in (e–f). Arrow indicates location of a hyperreflective structure that has similar appearance as microglia (central soma and radiating processing). *En-face* slices: (b) 8.2 μm below the ILM, (c) at the approximate mid-point of the NFL (25.3 μm below the ILM), and (d) at the base of the NFL (49.3 μm below the ILM). Cross-sectional views: (e) vertical and (f) horizontal through the OCT volume corresponding to the dashed lines shown in (a). Dashed lines indicate the *en-face* planes shown in (a–d). Inset in (e) shows 2 × zoomed region of single Gunn's dot. Segmentation results are shown in (g) cross-sectional, (h) *en-face*, and (i) *en-face* binary views. Scalebars = 50 μm. Accompanying videos (media) captures entire volume.

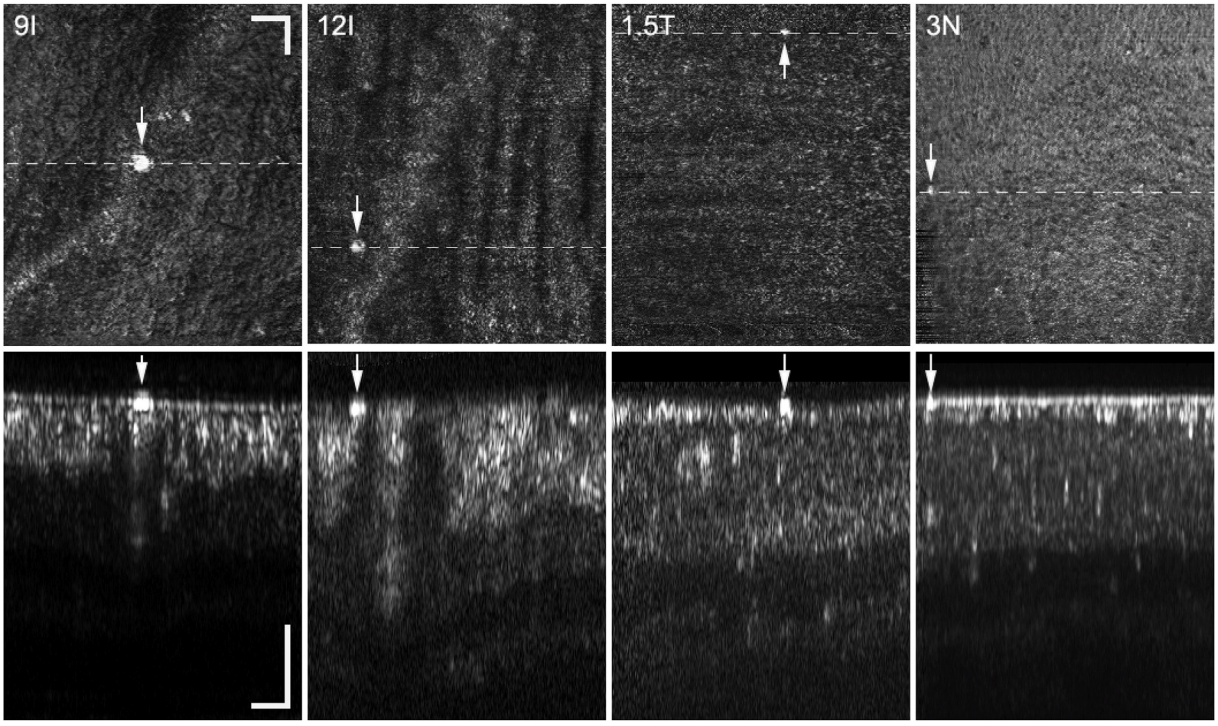

Fig. 3. *En-face* (top row) and cross-sectional (bottom row, lateral location of dashed line) AO-OCT views of single Gunn's dots (arrows) in four different healthy subjects (aged 28–72 years) at the retinal eccentricity indicated. *En-face* sections were maximum projections over 10 pixels (6.85 μm) centered on the ILM. Scalebars = 50 μm.

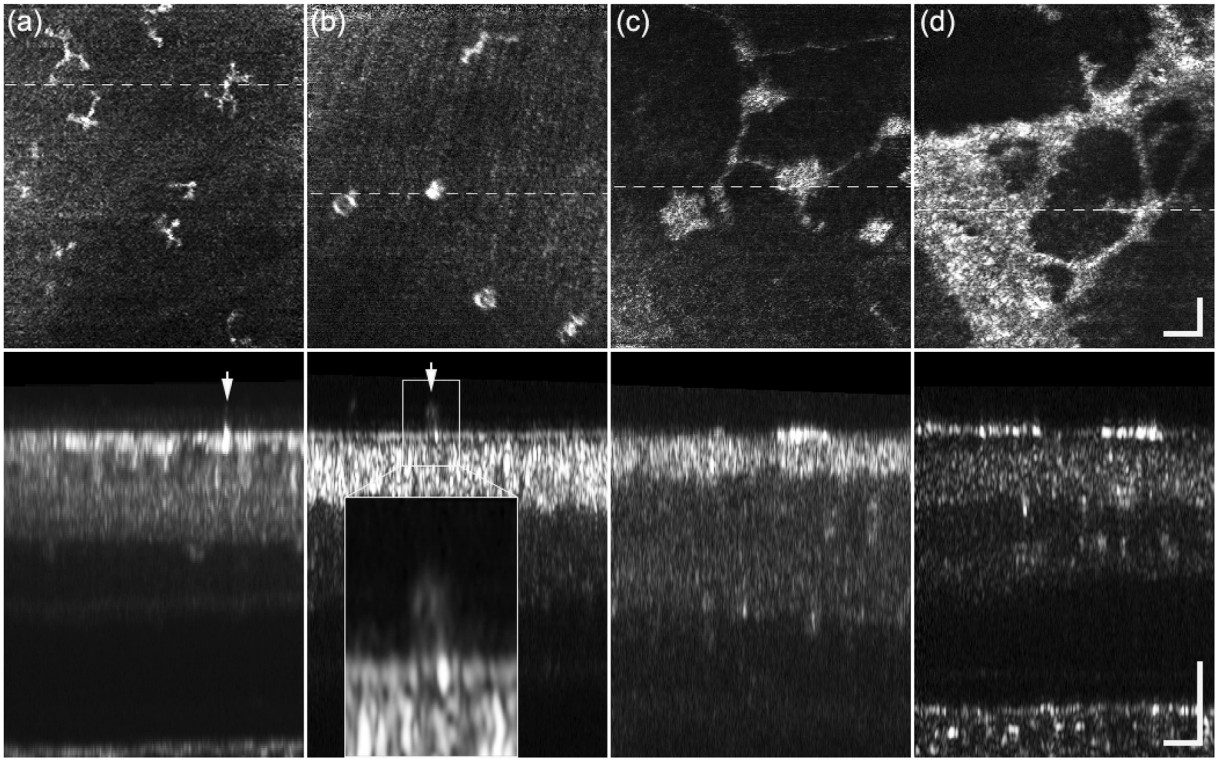

Fig. 4. *En-face* (top row) and cross-sectional (bottom row) AO-OCT views of: (a) Relatively dense region of ILM microglia in a 28-year old healthy subject, (b) ILM microglia in various stages of activation in a 58-year old healthy subject, (c) cellular hyperreflective structures in a 72-year old healthy subject and (d) cellular hyperreflective structures in a 54-year old subject with glaucoma. AO-OCT *en-face* projections are at a depth just above the ILM. Inset of cross-sectional view in (a) shows 3 × zoomed view of activated microglia. Scalebars = 50 μm.

such that it is unresolved and extremely low contrast, even for highly averaged AO-OCT cross-sections. However, there is no evidence in any of the AO-OCT cross-sections or *en-face* views examined in this study that the Gunn's dots are structurally connected to other cellular components within the retinal layers. Third, a recent study on the optical properties and waveguiding capabilities of Müller cells indicates that they are low reflection structures that waveguide light from the inner retina to the photoreceptors.[12] This is incompatible with all observations of Gunn's dots to date, including this study, where they appear as highly back-reflective and have been described to 'behave optically as small mirrors … '.[2] Finally, there is the question as to the relative density of Müller cells and Gunn's dots and why Gunn's dots appear preferentially in certain areas where Müller cells may be more uniformly and densely distributed across the retina.[5] If Gunn's dots are Müller cell end-feet, why are they not uniformly resolved across the entire retina at the same density as Müller cells? It may be possible that Gunn's dots are a pathological manifestation or sub-class of Müller cell end-feet, though this is unlikely for the other reasons listed above.

The localization of Gunn's dots within the ILM also makes it less likely that they are hyalocytes or associated with hyalocyte function. Hyalocytes typically reside in the vitreous humor at an average distance of 50 μm above the ILM.[6] Hyalocytes are typically 3–5 μm in diameter, smaller than measurements of Gunn's dots made here and elsewhere.[6,13] Also, the turnover rate of vitreous macrophages and hyalocytes is on the order of a week to several months[6,13,14] whereas previous measurements of Gunn's dots showed stable patterns of months to years, as indicated in Figs. 1 and 2 and previously.[2]

If the evidence from cross-sectional examination of Gunn's dots indicates that they are not likely to be Müller cell end-feet or hyalocytes, is there other evidence from the AO-OCT images that point to their origin and function? The results from our patients give some clues. Generally, the approximate co-localization near the ILM with microglia indicate that they may be associated with those particular glial cells. Along with Müller cells and astrocytes, microglia are the third basic type of retinal glial cells.[15–18] Whereas Müller cells extend across the inner retina in depth and astrocytes are predominantly confined to the NFL, microglia reside in the inner and outer plexiform layers (IPL and OPL), as well as smaller samples of cells at the ILM.[15] Microglia are known to migrate both laterally within their layers but also axially between layers.[18] Recently, glia cells have been resolved at the ILM in human subjects with high contrast and without exogenous dyes using AO-OCT,[9,19,20] probably owing to the large refractive index differential between vitreous humor and cellular structures. Microglia haven't been resolved in the IPL or OPL in humans, known to be their primary site of residence from animal studies.[16] One of the main roles of retinal microglia is phagocytosis of metabolic waste and pathological debris. We hypothesize that Gunn's dots are associated with glial function (e.g., corpora amylacea[21]), either the end-product of phagocytosis, or dead glia cells, formerly in their reactive, ameboid shape, that have fulfilled their function. One piece of counter-evidence is that microglia in their resting (ramified) state typically sit above the ILM and astrocytes in the NFL, whereas we have shown Gunn's dots to be confined to the ILM. However, microglia axial location changes with migration and activation state. Interestingly, microglia have recently been shown to play a role in NFL astrocyte phagocytosis,[22] which would explain the location of Gunn's dots in areas with a thick nerve fiber layer. ILM ramified microglia in one healthy subject are shown in Fig. 4(a). In another healthy subject, we have apparently captured a region that contains several microglia in various states of activation (Fig. 4(b)), from resting (central soma and radiating processes), to partially activated (retracted processes), to more fully activated (ameboid shape). The cross-sectional image in Fig. 4(b) through the center of the most activated microglia shows hyperreflectivity in the ILM near the portion or processes of the microglia in contact with the ILM. Other evidence that microglia may be related to Gunn's dots includes the presence of large quantities of debris-like structures at the ILM in older eyes (Fig. 4(c)) and eyes with glaucoma (Fig. 4(d)). Interestingly, in older and glaucoma subjects, there is a lack of OCT signal arising from the ILM compared to healthy subjects ((Fig. 4(c) and (d)). However, this hypothesized association runs counter to evidence that Gunn's dots are prevalent in adolescent eyes and that their density decreases with age. Further studies are required to test this hypothesis of the etiological origins of Gunn's dots.

The final questions regarding Gunn's dots relate to their correlation with pathological changes in the retina and potential use as a diagnostic or predictive biomarker for retinal disease. The high density of dots in adolescence, their ubiquitous presence in adult macula, as well as their chronic stability have pointed to a benign nature. However, their presence in areas of thicker NFL indicate a more complex function. Our patient is a glaucoma suspect with some retinal thinning in the same areas where the Gunn's dots are found (Fig. 1). Microglia are also relatively benign in the resting state but predictive of pathology as first responders to CNS injury. Studies of Gunn's dots in diseased eye, both early and late stage, is clearly needed to determine if they can serve as a biomarker of retinal disease.

5. Conclusions

AO-OCT imaging identified the axial location of Gunn's dots to be within the inner limiting membrane of the retina. Gunn's dots are mostly likely not Müller cell end-feet or hyalocytes. They may be associated with microglia or astrocyte activity since a portion of retinal microglia are found near the ILM and retinal astrocytes reside in the NFL. Further studies are required to determine if they are benign or a by-product of cellular activity that can be used as a biomarker for disease pathogenesis.

Patient consent

Written consent was obtained from all subjects to publish AO and clinical images. The report does not contain any personal information that could lead to the identification of the patient.

CRediT authorship contribution statement

Daniel X. Hammer: Conceptualization, Methodology, Software, Investigation, Writing - original draft, Writing - review & editing, Visualization. **Zhuolin Liu:** Methodology, Software, Investigation, Writing - review & editing. **Jenna A. Cava:** Data curation, Writing - review & editing. **Joseph Carroll:** Investigation, Conceptualization, Data curation, Writing - review & editing. **Osamah Saeedi:** Writing - review & editing.

Declaration of competing interest

Dr. Carroll received non-financial support from Optovue, Inc, grants from AGTC, personal fees and non-financial support from Meira GTx, and personal fees from Translational Imaging Innovations outside the scope of the submitted work. Dr. Saeedi received personal fees and non-financial support from Heidelberg Engineering, and a grant from Vasoptic Medical Inc. outside the scope of the submitted work.

Acknowledgments

The authors thank Christine A. Curcio and Wai T. Wong for helpful suggestions. Funding: This study was supported by an FDA Critical Path Initiative (CPi) Grant and a NIH Career Development Grant (K23EY025014). The investigation was conducted in part in a facility constructed with support from a Research Facilities Improvement Program, grant number C06RR016511 from the National Center for Research Resources, NIH. Its contents are solely the responsibility of the authors and do not necessarily represent the official views of the NIH.

Additional support from The Gene and Ruth Posner Foundation and the Thomas M. Aaberg, Sr. Retina Research Fund.

Appendix A. Supplementary data

Supplementary data to this article can be found online at https://doi.org/10.1016/j.ajoc.2020.100757.

Authorship

All authors attest that they meet the current ICMJE criteria for authorship.

Disclaimer

The mention of commercial products, their sources, or their use in connection with material reported herein is not to be construed as either an actual or implied endorsement of such products by the U.S. Department of Health and Human Services.

References

1. Gunn M. Peculiar appearance in the retina in the vicinity of the optic disc occurring in several members of the same family. *Tr Ophthalmol Soc UK*. 1883;3:110–113.
2. Paques M, Miloudi C, Kulcsar C, Leseigneur A, Chaumette C, Koch E. High-resolution imaging of Gunn's dots. *Retina.* 2015;35:120–124.
3. Boberg-Ans LC, Munch IC, Larsen M, Gopinath B, Wang JJ, Mitchell P. Gunn's dots in retinal imaging of 2,286 adolescents. *Retina.* 2017;37:382–387.
4. Paton L. Gunn's dots. *Br J Ophthalmol.* 1918;2:188–189.
5. Distler C, Dreher Z. Glia cells of the monkey retina – II. Müller cells. *Vis Res.* 1996;36(16):2381–2394.
6. Sakamoto T, Ishinashi T. Hyalocytes: essential cells of the vitreous cavity in vitreoretinal pathophysiology? *Retina.* 2011;31:222–228.
7. Dubra A, Sulai Y. Reflective afocal broadband adaptive optics scanning ophthalmoscope. *Biomed Optic Express.* 2011;2(6):1757–1768.
8. Scoles D, Sulai YN, Langlo CS, et al. In vivo imaging of human cone photoreceptor inner segments. *Invest Ophthalmol Vis Sci.* 2014;55(7):4244–4251.
9. Liu Z, Tam AJ, Saeedi O, Hammer DX. Trans-retinal cellular imaging with multimodal adaptive optics. *Biomed Optic Express.* 2018;9(9):4246–4262.
10. Scoles D, Higgins BP, Cooper RF, et al. Microscopic inner retinal hyper-reflective phenotypes in retinal and neurological disease. *Invest Ophthalmol Vis Sci.* 2014;55(7):4015–4029.
11. Burns SA, Elsner AE, Sapoznik KA, Warner RL, Gast TJ. Adaptive optics imaging of the human retina. *Prog Retin Eye Res.* 2019;68:1–30.
12. Franze K, Grosche J, Skatchkov SN, et al. Müller cells are living optical fibers in the vertebrate retina. *Proc Natl Acad Sci Unit States Am.* 2007;104:8287–8292.
13. van Meurs JC, Sorgente N, Gauderman WJ, Ryan SJ. Clearance rate of macrophages from the vitreous in rabbits. *Curr Eye Res.* 1990;9:683–686.
14. Qiao H, Hisatomi T, Sonoda KH, et al. The characterisation of hyalocytes: the origin, phenotype, and turnover. *Br J Ophthalmol.* 2005;89:513–517.
15. Kolb H. Glial cells of the retina. Accessed 10/11/2019 https://webvision.med.utah.edu/book/part-ii-anatomy-and-physiology-of-the-retina/glial-cells-of-the-retina/.
16. Singaravelu J, Zhao L, Fariss RN, Nork TM, Wong WT. Microglia in the primate macula: specializations in microglial distribution and morphology with retinal position and with aging. *Brain Struct Funct.* 2017;222:2759–2771.
17. Reichenbach A, Bringmann A. New functions of Müller cells. *Glia.* 2013;61(5):651–678.
18. Karlstetter M, Scholz R, Rutar M, Wong WT, Provis JM, Langmann T. Retinal microglia: just bystander or target for therapy? *Prog Retin Eye Res.* 2015;45:30–57.
19. Liu Z, Kurokawa K, Zhang F, Lee JJ, Miller DT. Imaging and quantifying ganglion cells and other transparent neurons in the living human retina. *Proc Natl Acad Sci Unit States Am.* 2017;114(48):12803–12808.
20. Kurokawa K, Crowell JA, Zhang F, Miller DT. Suite of methods for assessing inner retinal temporal dynamics across spatial and temporal scales in the living human eye. *Neurophotonics.* 2020;7(1):015013.
21. Woodford B, Tso MOM. An ultrastructural study of corpora amylacea of the optic nerve head and retina. *Am J Ophthalmol.* 1980;90:492.
22. Puñal VM, Paisley CE, Brecha FS, et al. Large-scale death of retinal astrocytes during normal development is non-apoptotic and implemented by microglia. *PLoS Biol.* 2019;17(10):e3000492 2019.